



Short communication

Preparation of LiFePO_4/C in a reductive atmosphere generated by windward aerobic decomposition of glucose

Shengping Wang, Chenggang Zhou, Quan Zhou, Gang Ni, Jinping Wu*

Sustainable Energy Laboratory, China University of Geosciences Wuhan, 388 Lumo road, Wuhan 430074, PR China

ARTICLE INFO

Article history:

Received 20 June 2010

Received in revised form 21 January 2011

Accepted 31 January 2011

Available online 26 February 2011

Keywords:

Lithium iron phosphate

Carbon coating

Glucose

Windward aerobic decomposition

ABSTRACT

We report the preparation of LiFePO_4/C electrode materials by thermal treating the hydrothermal LiFePO_4/C precursors in a reductive atmosphere from windward aerobic decomposition of glucose. XRD and ESEM characterization indicate that the procedure produces well carbon coated single-phase orthorhombic LiFePO_4 with small and evenly distributed particle-sizes. Comparing with the typical Ar/H_2 reductive atmosphere, samples from this procedure host larger initial discharge capacity (147.9 vs. 129.8 mAh g^{-1}) and excellent reversibility with a capacity reservation of 96.9% after 50 cycles at 0.1 C.

© 2011 Elsevier B.V. All rights reserved.

1. Introduction

Orthorhombic LiFePO_4 is one of the most promising electrode materials of lithium ion batteries for electric or hybrid electric vehicles. However, its low electrical and ionic conductivity restricted the electrochemical performance of batteries [1,2]. Intensive studies, such as doping metal ions (Ni [2], Zn [3], Al [4,5], Cu [4,6], Ti [4,7]), nonmetal ions (F [8] and Cl [9]), and most importantly, coating carbon on the particle surfaces [10–15], have been conducted to solve these issues. These efforts were proved to be impactful on improving the electronic and ionic conductivity of LiFePO_4 particles both intrinsically and exteriorly. The improvement brought by either doping or coating, in principle, depends largely on the preparation procedures and conditions. Hydrothermal method is the widely recognized technique yielding small and evenly distributed particle-sizes for LiFePO_4 [16–19], which had already been demonstrated to benefit the intrinsic ionic conductivity by reducing the Li^+ diffusion pathway straightforwardly. For purpose of carbon coating, carbon sources, mostly glucose [12,20–23], were introduced either into the hydrothermal solution or into the solid precursors. Liang et al. [20] discussed the two mixing mode and concluded that adding glucose in the solution gives higher initial discharge capacity of 154 mAh g^{-1} at 0.2 C. It is not strange that in solution glucose can be more homoge-

neously dispersed than physical mixing of solids. Consequently, better coating can be realized in the successive thermal treatment, where H_2 containing gas flow was always required to reduce the possible Fe(III) impurities from the hydrothermal stage. However, Fe(III) species, such as $\text{Li}_3\text{Fe}_2(\text{PO}_4)_3$ and Fe_2O_3 , were still observed in the thermal treated samples [24–26], which were harmful to the electrode performance [27]. It can be attributed to the fact that, the H_2 mixing gas is not sufficiently reductive to reduce these impurities. Increasing H_2 flow rate or sustaining reduction period theoretically should be able to overcome the problem. Unfortunately, loss of the thermal dissociated active carbon would occur since H_2 will react with carbon under such a condition. CO may be a proper candidate due to its stronger reductive capability to Fe(III) and inertia towards active carbon [24]. Chen and Yang [28] reported that $\text{Li}_3\text{Fe}_2(\text{PO}_4)_3$ and Fe_2O_3 can be fully converted to LiFePO_4 for 10 h at 550 °C with a CO flow rate of 5 mL min^{-1} . However, direct CO flow is inevitable to bring poisoning problems for operation in industry. To utilize the advance of CO, it is necessary to use appropriate CO atmosphere, rather than direct mixing of CO with inert gases, to achieve better reduction and carbon reservation.

In this paper, we prepared the LiFePO_4/C precursors via hydrothermal method. In the thermal treatment stage, we aerobically decomposed glucose at a windward position of the precursors in a tubular furnace to generate the CO atmosphere and prepared the LiFePO_4/C samples. For comparison, we also prepared samples by thermal treating the precursors in a typical Ar/H_2 atmosphere. The structural and morphological properties as well as the elec-

* Corresponding author. Tel.: +86 27 6788 3431; fax: +86 27 6788 3431.
E-mail address: itccms@cug.edu.cn (J. Wu).

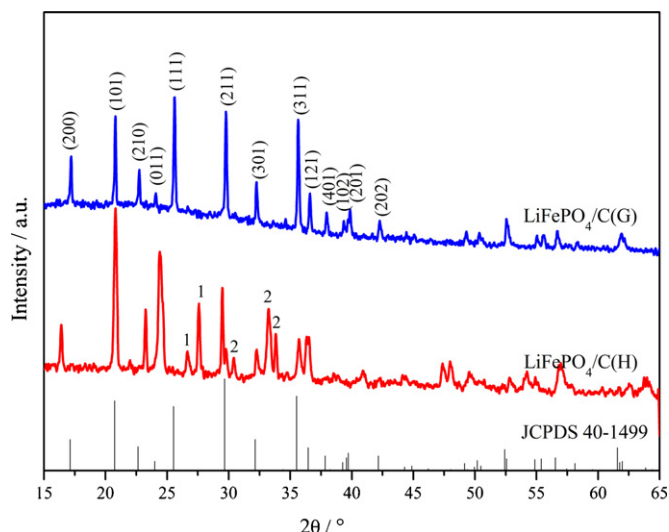


Fig. 1. X-ray diffraction patterns for $\text{LiFePO}_4/\text{C}(\text{G})$ and $\text{LiFePO}_4/\text{C}(\text{H})$, where marks "1" at $\text{LiFePO}_4/\text{C}(\text{H})$ curve represent Fe_2O_3 and "2" represent $\text{Li}_3\text{Fe}_2(\text{PO}_4)_3$.

Electrochemical performances of both samples were characterized and discussed.

2. Experimental

In our hydrothermal process, we used $\text{LiOH}\cdot\text{H}_2\text{O}$ (AR), $\text{FeSO}_4\cdot 7\text{H}_2\text{O}$ (AR) and H_3PO_4 (AR) as Li, Fe and P sources, respectively. A molar ratio 1:1:3 of LiOH solution (1 M), FeSO_4 solution (1 M) and H_3PO_4 (1 M) was firstly mixed. The glucose solution, with a gross glucose weight of 20 wt% to theoretical LiFePO_4 yield, was sequentially introduced into the mixture, which was reported to implement the best electrochemical performance of the product [29]. Each time 50 mL of the mixed solution were injected into a stainless hydrothermal reactor (inner lining of Teflon, volume 100 mL). The reaction was performed at 180°C for 5 h. The filtrated LiFePO_4/C precursors were washed using ultrapure water for 5 times and then dried in vacuum at 100°C for 1 h. In the thermal treatment step, we first used an Ar gas flow and the reducing agent is CO from the aerobic decomposition of glucose (200 g), which was put at 10 mm in windward to the precursors, and obtained sample labeled as $\text{LiFePO}_4/\text{C}(\text{G})$. Secondly, we thermal treated the precursors in a typical Ar/ H_2 (95/5 vol%) atmosphere and obtained sample $\text{LiFePO}_4/\text{C}(\text{H})$. Both the two procedures were processed in a quartz tubular furnace (tube diameter: 120 mm; tube length: 1000 mm) at 650°C for 6 h with a 5 mL min^{-1} gas flow rate.

The structure characterization of the two products was performed on an X'Pert PRO DY2198 X-ray diffractometer with $\text{Cu K}\alpha$ radiation ($\lambda = 1.54056\text{ \AA}$) using a curved graphite crystal monochromator. The surface morphology was characterized on a Quanta2000 Environmental scanning electron microscopy with an accelerating voltage of 30 kV and a vacuum degree of $1.33 \times 10^{-3}\text{ Pa}$.

The charge/discharge performance of the two samples was examined using the test coin cells. LiFePO_4/C powders, acetylene black and polytetrafluoroethylene (PTFE) with a weight ratio of 85:10:5 were evenly mixed and coated on an aluminum foil. The punched cathodes are round shaped with a diameter and thickness of 15 mm and 0.2 mm, respectively. The cathodes were dried at 200°C for 12 h in a vacuum oven before assembling to test cells. The anode was lithium metal and a mixed solvent EC, DMC and EMC with a volume ratio of 1:1:1 containing 1 M LiPF_6 was used as the electrolyte. The separator was celegrad 2300 microporous membrane. Test cells were assembled in an Ar-filled glove box at room temperature. The galvanostatic charge–discharge experiment was

performed at 0.1 C on a RF-T cell test system between 2.0 and 4.2 V (vs. Li/Li^+). Electrochemical impedance spectroscopy (EIS) and cyclic voltammetry (CV) were performed using a three-electrode cell with a counter-electrode and a reference-electrode both made of lithium. CV was carried out at a sweep rate of 0.5 mV s^{-1} and all measurements were performed in the voltage range of 3.1–4.0 V on an electrochemical workstation (CHI660C). EIS was carried out in the frequency range of 10^5 – 10^{-2} Hz with ac amplitude of 5 mV at a potential of 3.45 V.

3. Result and discussion

The typical peaks of standard orthorhombic LiFePO_4 pattern JCPDS40-1499 appeared in the XRD pattern of both $\text{LiFePO}_4/\text{C}(\text{H})$ and $\text{LiFePO}_4/\text{C}(\text{G})$, suggesting that each sample has well-grown olivine crystal structure, as shown in Fig. 1. However, for $\text{LiFePO}_4/\text{C}(\text{H})$, peaks of impurities such as $\text{Li}_3\text{Fe}_2(\text{PO}_4)_3$ and Fe_2O_3 were identified, implying uncompleted reduction of $\text{Fe}(\text{III})$ species, as reported by Goodenough and coworkers [24]. As expected, the CO reduced sample $\text{LiFePO}_4/\text{C}(\text{G})$ exhibited pure orthorhombic phase, suggesting all impurities were converted to final products. Carbon was deemed to be amorphous since there was no crystalline carbon peak in Fig. 1. Using gravimetric method, we noticed that the final composition of carbon in $\text{LiFePO}_4/\text{C}(\text{G})$ and $\text{LiFePO}_4/\text{C}(\text{H})$ is 4.83 wt% and 3.27 wt%, respectively. Apparently, better coating reservation was achieved when the precursors were reduced by CO. Another important clue is that, the feature peak intensity of $\text{LiFePO}_4/\text{C}(\text{G})$ is weaker than that of $\text{LiFePO}_4/\text{C}(\text{H})$, telling the fact that the particle growth in the formal case was restricted. It is not strange that, for $\text{LiFePO}_4/\text{C}(\text{H})$, the carbon loss leads to more direct contact of small LiFePO_4 particles, resulting in stronger Ostwald ripening towards larger particles. In fact, the ESEM image shown in Fig. 2 clearly shows that the $\text{LiFePO}_4/\text{C}(\text{G})$ particles are almost half-sized of $\text{LiFePO}_4/\text{C}(\text{H})$ (500 vs. 1000 nm, in average). Comparing with Fig. 2(b), Fig. 2(a) displayed smoother particle shape and evenly distributed particle-sizes. With better coating and appropriate size and shape, the CO reduced sample was consequently assumed to have better electrochemical properties.

Fig. 3(a) shows that the initial discharge capacity of $\text{LiFePO}_4/\text{C}(\text{G})$ and $\text{LiFePO}_4/\text{C}(\text{H})$ was 147.9 and 129.8 mAh g^{-1} , respectively, with the charge and discharge voltage platform of both two samples appeared at $\sim 3.5\text{ V}$ and $\sim 3.4\text{ V}$, respectively, corresponding to the $\text{Fe}^{2+}/\text{Fe}^{3+}$ redox couple. As in the CV experiments, the two redox potentials were also observed with the same values as shown in Fig. 3(b). The potential difference between oxidation and reduction peaks of $\text{LiFePO}_4/\text{C}(\text{G})$ was 0.134 V, smaller than that of $\text{LiFePO}_4/\text{C}(\text{H})$ (0.143 V), implying better electrode reversibility which should be attributed to the better coating of $\text{LiFePO}_4/\text{C}(\text{G})$. According to the EIS curves of the two samples shown in Fig. 4, the charge transfer resistance of $\text{LiFePO}_4/\text{C}(\text{G})$ and $\text{LiFePO}_4/\text{C}(\text{H})$ was $725.3\ \Omega$ and $1049.6\ \Omega$, respectively. Obviously, the substantially smaller charge transfer resistance of $\text{LiFePO}_4/\text{C}(\text{G})$ will decrease the Li^+ concentration difference between particle surface and interior-particle. As a consequence, the diffusion and reaction kinetics during the charge/discharge cycles were improved. With the method proposed by Liu et al. [3] and Prosini et al. [30], the Li^+ diffusion rate of $\text{LiFePO}_4/\text{C}(\text{G})$ was calculated to be $1.49 \times 10^{-13}\text{ cm}^2\text{ s}^{-1}$, quantitatively higher than that of $\text{LiFePO}_4/\text{C}(\text{H})$ ($1.30 \times 10^{-13}\text{ cm}^2\text{ s}^{-1}$). Consequently, better reversibility of $\text{LiFePO}_4/\text{C}(\text{G})$ can also be assumed comparing with $\text{LiFePO}_4/\text{C}(\text{H})$.

Finally, we performed 50 charge/discharge cycles for the two samples at 0.1 C and the results are shown in Fig. 5. Very little capacity attenuation was observed in the beginning 10 cycles for either sample. However, at the 50th cycle, $\text{LiFePO}_4/\text{C}(\text{G})$ still host

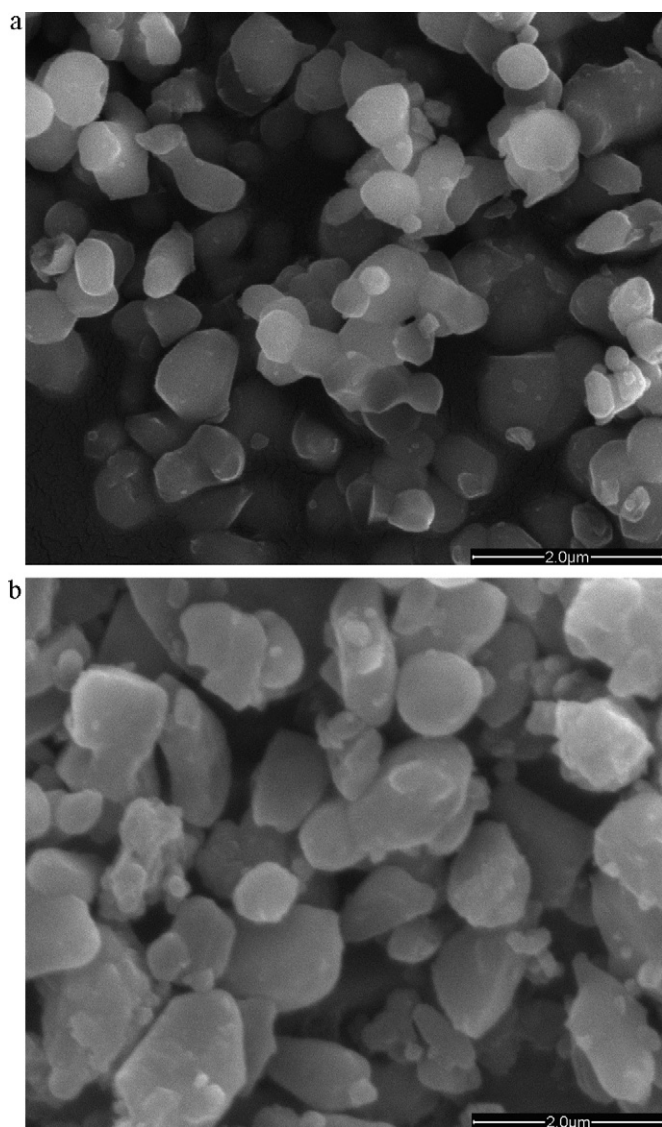


Fig. 2. ESEM micrograph for (a) LiFePO₄/C(G) and (b) LiFePO₄/C(H).

a discharge capacity of 143.3 mAh g⁻¹ (3.11% decay rate), comprehensively higher than that of LiFePO₄/C(H) (107.5 mAh g⁻¹, 16.41% decay rate). The first discharge capacity difference originated from the fact that impurity species in LiFePO₄/C(H) prevent the neighboring Li⁺ insertion and desertion. Since LiFePO₄/C(G) has smaller EIS, the lattice distortion and destruction caused by Li⁺ intercalation was minimized and the capacity loss was consequently weakened. On the other hand, more importantly, smaller and evenly distributed particle size of LiFePO₄/C(G) benefits the reservation of active sites by shortening the Li⁺ diffusion pathway, which is considerably critical to the reversibility of electrodes.

4. Conclusion

In this paper, we developed a new reducing technique to thermal treat the LiFePO₄/C precursors from hydrothermal process. By aerobically decomposing glucose at windward site of the precursors in tubular furnace, we obtained a CO containing reducing atmosphere which can completely convert the Fe(III) impurities to pure orthorhombic LiFePO₄ phase. In industry, the cost to prevent Fe²⁺ oxidation during hydrothermal stage is not as low as acceptable. Comparing with typical Ar/H₂ reduced samples, the

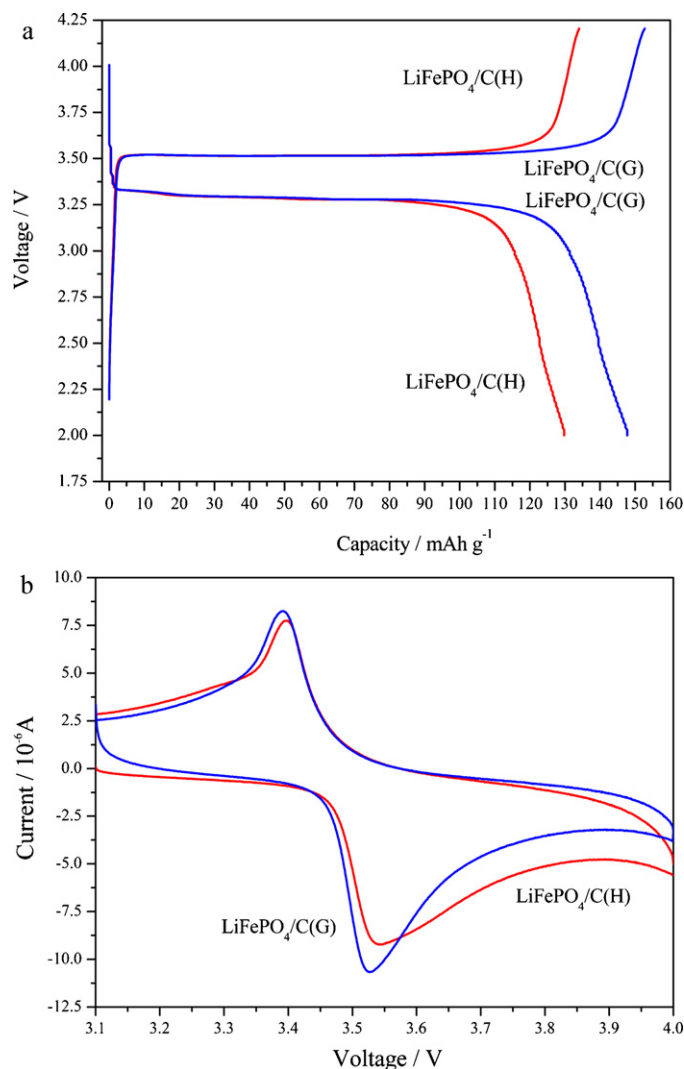


Fig. 3. The initial charge–discharge curves (a) and CV curves (b) of the samples.

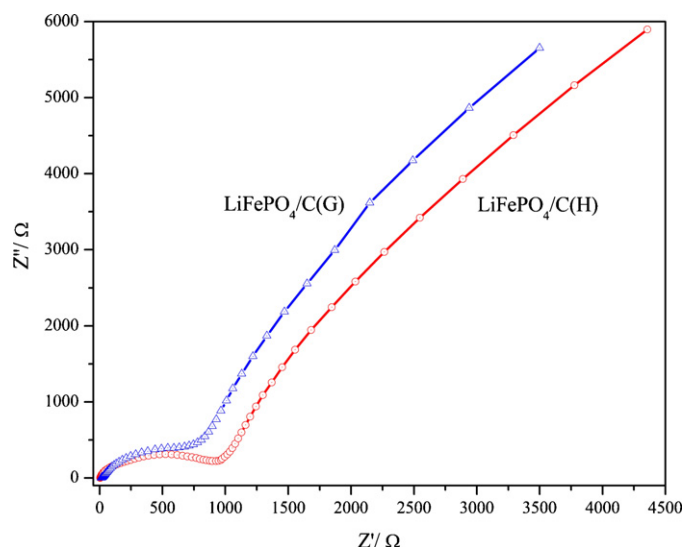


Fig. 4. EIS spectra of the samples.

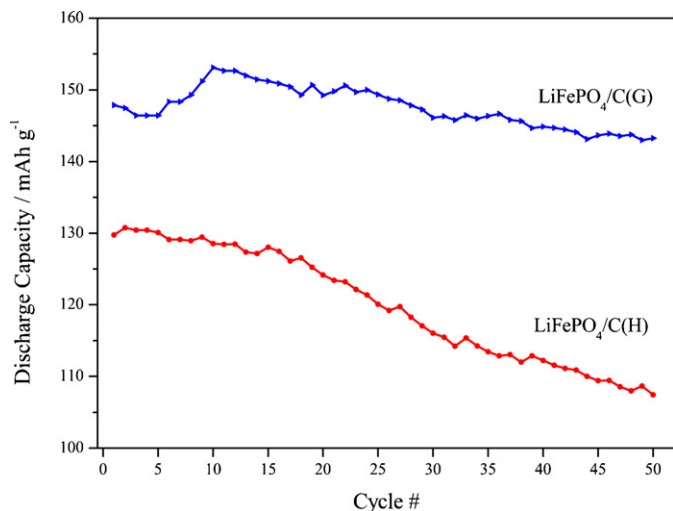


Fig. 5. The cycle performances of the samples at 0.1 C.

new technique rationally protected the coating layers resulting in smaller and evenly distributed particle sizes. Owing these properties, the product $\text{LiFePO}_4/\text{C}(\text{G})$ exhibited excellent electrochemical performance and electrode reversibility. This technique is relatively simple and safe and may be potentially applicable for industry.

References

- [1] A.K. Padhi, K.S. Nanjundaswamy, J.B. Goodenough, *J. Electrochem. Soc.* 144 (1997) 1188.
- [2] P.S. Herle, B. Ellis, N. Coombs, L.F. Nazar, *Nat. Mater.* 3 (2004) 147.
- [3] H. Liu, Q. Cao, L.J. Fu, C. Li, Y.P. Wu, H.Q. Wu, *Electrochem. Commun.* 8 (2006) 1553.
- [4] M. Abbate, S.M. Lala, L.A. Montoro, J.M. Rosolen, *Electrochem. Solid State Lett.* 8 (2005) A288.
- [5] J. Xu, G. Chen, Y.J. Teng, B. Zhang, *Solid State Commun.* 147 (2008) 414.
- [6] R. Yang, X.P. Song, M.S. Zhao, *J. Alloys Compd.* 468 (2009) 365.
- [7] G.X. Wang, S. Bewlay, S.A. Needham, H.K. Liu, R.S. Liu, V.A. Drozd, J.F. Lee, J.M. Chen, *J. Electrochem. Soc.* 153 (2006) A25.
- [8] L. Yang, L.F. Jiao, Y.L. Miao, H.T. Yuan, *J. Solid State Electrochem.* 14 (2010) 1001.
- [9] L. Yang, L.F. Jiao, Y.L. Miao, H.T. Yuan, *J. Solid State Electrochem.* 13 (2009) 1541.
- [10] X.Z. Liao, Z.F. Ma, Q. Gong, Y.S. He, L. Pei, L.J. Zeng, *Electrochem. Commun.* 10 (2008) 691.
- [11] M. Konarova, I. Taniguchi, *Powder Technol.* 191 (2009) 111.
- [12] Z.R. Chang, H.J. Lv, H.W. Tang, H.J. Li, X.Z. Yuan, H.J. Wang, *Electrochim. Acta* 54 (2009) 4595.
- [13] H. Huang, S.C. Yin, L.F. Nazar, *Electrochem. Solid State Lett.* 4 (2001) A170.
- [14] A.D. Spong, G. Vitins, J.R. Owen, *J. Electrochem. Soc.* 152 (2005) A2376.
- [15] S.T. Myung, S. Komaba, N. Hirosaki, H. Yashiro, N. Kumagai, *Electrochim. Acta* 49 (2004) 4213.
- [16] S.F. Yang, P.Y. Zavalij, M.S. Whittingham, *Electrochem. Commun.* 3 (2001) 505.
- [17] S.F. Yang, Y.N. Song, P.Y. Zavalij, M.S. Whittingham, *Electrochem. Commun.* 4 (2002) 239.
- [18] A. Kuwahara, S. Suzuki, M. Miyayama, *J. Electroceram.* 24 (2010) 69.
- [19] J.F. Ni, M. Morishita, Y. Kawabe, M. Watada, N. Takeichi, T. Sakai, *J. Power Sources* 195 (2010) 2877.
- [20] G.C. Liang, L. Wang, X.Q. Ou, X. Zhao, S.Z. Xu, *J. Power Sources* 184 (2008) 538.
- [21] A.F. Liu, Z.H. Hu, Z.B. Wen, L. Lei, *J. An. Ionics* 16 (2010) 311.
- [22] H.L. Zou, G.H. Zhang, P.K. Shen, *Mater. Res. Bull.* 45 (2010) 149.
- [23] L. Wang, G.C. Liang, X.Q. Ou, X.K. Zhi, J.P. Zhang, J.Y. Cui, *J. Power Sources* 189 (2009) 423.
- [24] A.A. Salah, A. Mauger, K. Zaghib, J.B. Goodenough, N. Ravet, M. Gauthier, F. Gendron, C.M. Julien, *J. Electrochem. Soc.* 153 (2006) A1692.
- [25] F. Gao, Z. Tang, J. Xue, *J. Univ. Sci. Technol. Beijing* 15 (2008) 802.
- [26] K.S. Hong, S.M. Yu, M.G. Ha, C.W. Ahn, T.E. Hong, J.S. Jin, H.G. Kim, E.D. Jeong, Y.S. Kim, H.J. Kim, C.H. Doh, H.S. Yang, H. Jung, *Kor. Chem. Soc.* 30 (2009) 1719.
- [27] C.M. Julien, A. Mauger, A. Ait-Salah, M. Massot, F. Gendron, K. Zaghib, *Ionics* 13 (2007) 395.
- [28] Y.H. Chen, Y. Yang, *Electrochemistry* 14 (2008) 388.
- [29] Z.Y. Chen, H.L. Zhu, S.J.R. Fakir, V. Linkov, *Solid State Ionics* 179 (2008) 1810.
- [30] P.P. Prosini, M. Lisi, D. Zane, *Solid State Ionics* 148 (2002) 45.